

Correlation Analysis for Fault Detection Statistics in Integrated GNSS/INS Systems

Jinling Wang¹, Ali Almagbile¹, Youlong Wu¹ and Toshiaki Tsujii²

¹School of surveying and Geospatial Engineering, University of New South Wales, Sydney, NSW 2052, Australia.

²High-Precision Satellite Navigation Technology Section; Aviation Program Group, Japan Aerospace Exploration Agency (JAXA), Tokyo, Japan

Abstract

Global Satellite Navigation Systems (GNSS) have been widely used for positioning, navigation and timing (PNT). Therefore, the integrity of the satellite based navigation systems has been a major concern for many liability critical applications, such as civil aviation, and location-based services (LBS). Over the past two decades, GNSS Receiver Autonomous Integrity Monitoring (RAIM) procedures have been developed, but the efficiency of such procedures is highly dependent on measurement redundancy and geometric strength within the GNSS positioning solutions. Reliability of a PNT system can be measured by, not only the well-known Minimal Detectable Biases (MDBs), but also the recently derived Minimal Separable Biases (MSBs) for the measurements. While the previous research has shown that the MSBs are directly related to the correlations between the faulty measurement detection statistics, a comprehensive analysis for such correlations between fault (or outlier) detection statistics is still lacking, even for commonly used GNSS/INS integration scenarios. In this research, we have demonstrated that with the aid of inertial sensors, even with low-cost MEMS sensors, the MDBs and correlation coefficients between the measurement fault detection statistics can be significantly reduced, thus improving the separability of faults in GNSS measurements.

Keywords: GNSS, GNSS/INS Integration, Fault Detection and Identification, Separability, Correlation Analysis

1. Introduction

As more and more human activities are relying on the use of satellite navigation technologies, the integrity of satellite navigation solutions has become a major issue, especially for the life-safety-critical and liability-critical applications. Therefore, a reliable integrity monitoring

procedure must be used to eliminate hazardous and misleading navigation information caused by failure(s) within the navigation system and provide a timely warning message to the user if the navigation information is not good enough for certain applications at a specific time. One effective approach to address the satellite navigation integrity risks is the so-called Receiver Autonomous Integrity Monitoring (RAIM).

The RAIM strategy is based on the consistency check among satellite pseudo-range measurements used in a navigation solution. If a faulty measurement/satellite (failure) is detected, a procedure may be activated to identify and exclude the failure from the navigation solution, which will therefore remain fault-free and reliable for use in the defined applications. Thus, a RAIM procedure is self-contained and can be used as the ultimate integrity monitor (e.g., Wang and Ober, 2009; Wang and Kubo, 2000).

If measurements are contaminated by faults/outliers, the user position solution may exceed the predefined allowable accuracy range. If so, the role of RAIM comes to provide a warning message (alarm) to the user within a given period of time that the system must not be used for navigation (Ochieng *et al.*, 2002). If RAIM fails to provide measurement check (mis-detection) when failure occurs or falsely warn the user (false alarm) that the system should not be used for navigation, the navigation will be in risk. However, the performance of RAIM depends on the number of visible satellites to the user, the strength of geometry and the accuracy of the pseudo-range measurements. For instance, when the number of visible satellites is five, RAIM can provide a detection of the fault, but the fault is inseparable due to the full correlation between fault detection statistics (Hewitson and Wang, 2007; Wang and Knight, 2012).

Although RAIM can provide an acceptable confidence level for the user with the status of navigation solutions, the design of RAIM is limited to detect one fault at a

time. When the system encounter more than one failure at a time, the capability of RAIM degrades or even stops to provide any reliable integrity monitoring for the system. As a result, several investigations (e.g., Wang and Chen, 1999; Knight *et al.*, 2010) have developed methods for detecting and identifying multiple simultaneous faults in either standalone navigation systems or integrated navigation systems.

However, the reliability of RAIM procedure is highly dependent upon sufficient satellite redundancy in the navigation solutions, as well as the strong geometry of visible satellites. But such conditions may not be guaranteed under poor environments, such as in city canyons, where majority of business activities are located. This issue can be addressed through robust integration between various GNSS satellite navigation systems and between GNSS and other complementary navigation sensors, such as pseudo-satellites (e.g., Wang, 2002) and/or Inertial Navigation System (INS) (e.g., Wang *et al.*, 2003).

In integrated GNSS/INS navigation systems, fault detection and identification has been well documented in the literature. Sturza (1989) presented a fault detection algorithm based on hypothesis testing in parity space while Teunissen (1990) investigated quality control of integrated navigation systems using innovation and recursive filtering. An innovation based autonomous integrity monitoring extrapolation (AIME) was presented by Diesel and King (1995). Brenner (1995) used Kalman Filter (KF) to quantify the performance of integrity monitoring. Nikiforve (2002) presented fault detection and exclusion in multi-sensor integration based on KF innovations. Hewitson and Wang (2010) investigated the quality control for integrated GNSS and inertial navigation systems.

It has been widely accepted that integration of GNSS/INS offers great advantages because the characteristics of both sensors complement each other. One of these advantages is that through the integration, the integrity and reliability of the navigation solution can be improved. Integrity and reliability are two parameters that are closely connected. While integrity refers to the ability of the system to provide a warning message to the user when the system must not be used for navigation, the reliability is the ability of the system to detect the faults (or outliers) in the measurements, hence evaluating the impact of undetected faults on the positioning solution (O'Keefe, 2001).

It is obvious that detection and identification of single and multiple faults has been given considerable attention by many researchers. However, most of the investigations that dealt with fault exclusion/separation in either geodetic surveying or navigation applications are limited to the single fault case. Förstner (1983) developed the

separability measures to separate the "good" measurements from the contaminated one. The separability measures are based on correlation coefficients between faulty measurement detection statistics. The higher the correlation coefficients between tests statistics, the less likely the system can separate the fault. In other words, due to the high correlation coefficients between fault detection statistics, several measurements may have a large value for their associated detection statistics, even when there is only one fault, increasing the linkelihood to identify a wrong measurement as a fault. The separability measures are employed to evaluate the capability of the system to separate any pair of the fault detection statistics. In GNSS applications, an analysis of outlier separability measures under different numbers of visible satellites and various satellites geometries was investigated by Hewitson and Wang (2006); Wang and Knight (2012), while Almagbile and Wang (2011) and Almagbile *et al.* (2011) evaluated outlier separability measures in integrated GPS/INS systems. This evaluation considered the factors such as the number of visible satellites, satellites geometry and the number of system states models that influences the correlation coefficients between fault detection test statistics. However, such analysis was based on a specific epoch (snapshot) results for the case of single fault.

Using the same principles of single outlier separability case, multiple faults separability measures were discussed by Förstner (1983) and Li (1986). In this case multi-dimensional correlation coefficients were employed as an indicator of the capability of the system to separate the true hypothesis from the false alternative hypotheses in photogrammetric adjustment applications..

In this paper, we will present a comprehensive correlation analysis for the faulty measurement detection statistics in integrated GNSS/INS systems. The structure of the paper is as follows: Section 2 discusses the quality control of integrated GNSS/INS systems including statistical quality control procedures for detection and identification for single and multiple faults. Section 3 presents simulated studies on the correlation analysis for the fault detection statistics in various GNSS and GNSS/INS integration scenarios, which will be followed by the concluding remarks in Section 4.

2. Quality Control for GNSS/INS Integration

In the next generation GNSS receivers, measurements from multiple satellite constellations are combined to improve the integrity of navigation solutions. However, to integrate the measurements from two or more satellite constellations, the clock-offsets between the constellations need to be treated properly. Options of such treatments may include: a) adding GNSS system

time-offsets as unknown parameters into the navigation solution; or b) measuring/broadcasting precise time-offset values which could be considered as errorless or as pseudo-measurements (Wang et al., 2011). For example, the GPS/QZSS system time offset has been dealt with at the system level, and thus, users will not estimate this time offset in their navigation solutions.

In a GNSS-only system, faulty measurement detection and identification is normally carried out with a so-called snapshot least squares framework. Such a procedure should be implemented through a Kalman filter for GNSS/INS integration where the dynamic information captured by the INS sensors can be efficiently used. In fact, the Kalman Filter can also be presented as a least-squares procedure in each epoch (Sorenson, 1970; Salzmann, 1993; Wang et al., 1997; 2008).

Mathematically, the discrete time of the system state and measurement model of the Kalman filtering can be written as follows:

$$x_k = \Phi_{k-1}x_{k-1} + w_{k-1} \quad (1)$$

$$z_k = H_k x_k + v_k \quad (2)$$

where x_k is the $(n \times 1)$ state vector, Φ_k is the $(n \times n)$ transition matrix, z_k is the $(r \times 1)$ measurements vector, H_k is the $(r \times n)$ measurement (or design) matrix. The variables w_k and v_k are the uncorrelated white noise errors with covariance matrices Q_k and R_k respectively. Then equations (1) and (2) can be integrated as follows:

$$l_k = \begin{bmatrix} z_k \\ \bar{x}_k \end{bmatrix}, A_k = \begin{bmatrix} H_k \\ E \end{bmatrix}, v_k = \begin{bmatrix} v_{zk} \\ v_{\bar{x}k} \end{bmatrix} \quad (3)$$

$$\text{i.e.,} \quad l_k + v_k = A_k x_k \quad (4)$$

where E is the $(m \times m)$ identity matrix and \bar{x}_k is the vector of the predicted states at epoch k . The variance-covariance matrix C_{l_k} , which is derived from both the measurement noise covariance matrix R_k and the covariance matrix \bar{P}_k of the predicted states within the Kalman filtering, can be written as (Wang et al., 1997):

$$C_{l_k} = \begin{bmatrix} R_k & 0 \\ 0 & \bar{P}_k \end{bmatrix} = P^{-1} \quad (5)$$

where P is the weight matrix with the priori variance factor being assigned as one. The optimal estimates of the state parameters \hat{x}_k and their covariance matrix $Q_{\hat{x}_k}$ can be written as:

$$\hat{x}_k = (A_k^T P A_k)^{-1} A_k^T P l_k \quad (6)$$

$$Q_{\hat{x}_k} = (A_k^T P A_k)^{-1} \quad (7)$$

The KF residuals v_k and the associated cofactor Q_{v_k} can be written as:

$$v_k = \begin{bmatrix} v_{zk} \\ v_{\bar{x}k} \end{bmatrix} = A_k \hat{x}_k - l_k \quad (8)$$

$$Q_{v_k} = C_{l_k} - A_k Q_{\hat{x}_k} A_k^T \quad (9)$$

where the symbol k is used as a notation for the current epoch and it will be ignored throughout this paper for simplification. By performing the KF as least squares, many existing faulty measurement detection and identification procedures for GNSS can also be used in the integrated GNSS/INS systems.

2.1. Faulty measurement detection statistics

For the case of single faulty measurement, the w -test can then be used to identify the corresponding measurement, where the test statistic is (e.g., Baarda, 1968; Teunissen, 1990; Wang and Chen, 1999)

$$w_i = \frac{-e_i^T P v}{\sqrt{e_i^T P Q_v P e_i}} \quad (10)$$

where e_i is a vector in which the i th element is equal to one and all other elements are equal to zero. Under the null hypothesis, w_i has a standard normal distribution and under the alternative, w_i has the following non-centrality

$$\delta_i = \nabla S_i \sqrt{e_i^T P Q_v P e_i} \quad (11)$$

where ∇S_i is the size of the fault in the i th measurement. The critical value for the test is $N_{1-\alpha/2}(0,1)$, where α is the significance level.

The Minimal Detectable Bias (MDB) specifies the lower bound for detectable fault (outlier) with a certain probability and confidence level. The MDB is determined as (Baarda, 1968; Teunissen, 1990; Wang and Chen, 1999)

$$\nabla_0 S_i = \frac{\delta_0}{\sqrt{e_i^T P Q_v P e_i}} \quad (12)$$

where δ_0 is the non-centrality parameter, which depends on the chosen power of the test $(1 - \beta)$ and significance level or false alarm rate (α) .

For the cases of multiple faulty measurements, regardless the true number of faults (outliers) that exist in the

measurements, the faulty measurement detection statistic can be written as follows (e.g., Teunissen, 1990; Wang and Chen, 1999; Knight *et al.*, 2010):

$$T_i^2 = \frac{l^T P Q_v P G_i (G_i^T P Q_v P G_i)^{-1} G_i^T P Q_v P l}{\sigma_0^2} \quad (13)$$

where σ_0^2 the priori variance factor assigned as one in this paper; G_i is an n by θ matrix, with rank θ , containing zeros with a "1" in each column corresponding to the faults. The statistic T_i^2 has a Chi-square distribution with θ as the degrees of freedom. Fault identification based on Equation (13) can be applied for different number of outliers, such as two or three outliers. In this study, we consider the case that two outliers exist in the measurements. In this case θ is equal to 2 and the G_i matrix takes the following form:

$$G_i^2 = \begin{bmatrix} 0 & 0 & \cdot & 1 & 0 & 0 \\ 0 & 0 & 0 & \cdot & 1 & 0 \end{bmatrix}^T \quad (14)$$

All the possible T_i^2 may be presented as the $(n \times \theta)$ matrix corresponding to the G_i matrix.

Similar to the single fault case, the minimal detectable bias can also be derived for the case of multiple faults, but with very complicated formulae as such MDBs are multiple dimensional, see the details in, e.g., Wang and Chen, (1999), Knight *et al.* (2010).

2.2. Correlation coefficients between the fault detection statistics

In the fault detection process, the largest fault detection statistic (in absolute value) is associated with the most likely faulty measurement. However, due to the correlation between this statistic and any other fault detection statistics, one fault may result in many fault statistics being close each other. Therefore, such correlation coefficients are closely related to the fault separability (e.g., Forstner, 1983; Li, 1986; Wang and Knight, 2012). In order to ensure any two alternatives are separable, such correlation coefficients should be small.

The correlation coefficient between two single fault detection statistics is given below (e.g., Förstner, 1983; Hewitson and Wang, 2007)

$$\rho_{ij} = \frac{e_i^T P Q_v P e_j}{\sqrt{e_i^T P Q_v P e_i} \cdot \sqrt{e_j^T P Q_v P e_j}} \quad (15)$$

In this paper, the absolute value of ρ_{ij} is considered. The bigger the correlation between two test statistics, the more difficult they are to separate.

For the multiple faults case, the fault detection statistics T_i^2 and T_j^2 are for two groups of faulty measurements, e.g., Group i and Group j . In the two fault case, these two groups are actually two pairs of measurements, for example, measurement pairs (2, 4) and (3,5).

Similarly, multiple fault separability may also be related to the correlation between two fault vectors associated with the two groups of measurements to be tested. For convenience, the maximum correlation and the global correlation are derived as follows (Förstner, 1983; Li, 1986):

$$(Q_{ij})_{\max} = \sqrt{\lambda_{\max}(M_{ij})} \quad (16)$$

$$M_{ij} = (p_{ij})^{-1} \cdot (p_{ij}) \cdot (p_{ij})^{-1} \cdot (p_{ij}) \quad (17)$$

$$p_{ij} = G_i^\theta P Q_v P G_j^\theta \quad (18)$$

where $(\lambda_{\max}(M_{ij}))$ is the maximum eigenvalue of matrix (M_{ij}) . The rank of this matrix is the same as the number of faults to be detected. And G_i^θ and G_j^θ correspond to the faults tests (i and j), respectively. The examples of them are given by Equation (14)

The global correlation coefficients can also be computed as follows (e.g., Li, 1986):

$$(Q_{ij})_{Global} = \frac{tr(M_{ij})}{\sqrt{r_i \cdot r_j}} \quad (19)$$

where r_i and r_j are the degrees of freedom for T_i^2 and T_j^2 , respectively.

3. Simulated Data Sets for GNSS and INS Trajectory

In this research, GNSS and INS data simulations as well as the tight GNSS/INS integration data processing were based on GPSOft® Satellite Navigation, Inertial Navigation System, Navigation System Integration and Kalman Filter Toolbox. This software has been modified to include reliability and correlation analysis functionalities for use in this study. The simulation process is divided into two steps:

Firstly, as shown in Fig. 1, a reference trajectory was created through a moving receiver by using initial position, initial velocity and initial attitude.

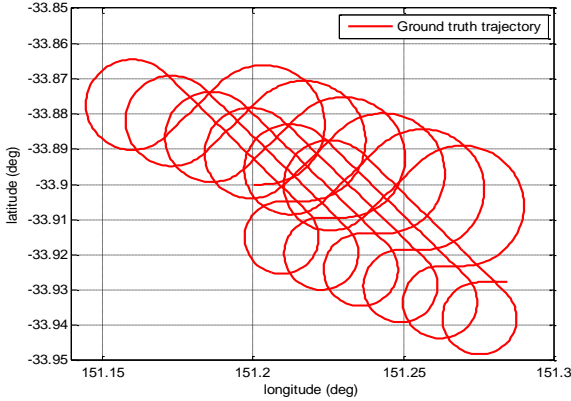


Figure 1: Simulated vehicle trajectory

Then the INS delta velocity and delta theta were created for a selected site in Sydney. The geodetic coordinates of the selected location are 33° 55 04”S, 151° 13’ 55”E, with an elevation of 87m above the sea level. The MEMS, Tactical and Navigation grade INS data sets were simulated with an output rate of 200Hz along with simulated initial alignment, velocity error and gyros and accelerometer biases. The details for IMU sensor noise parameters used in the simulations are listed in Table 1.

Table 1: IMU Noise Parameters for Simulations

IMU Grades	Accelerometers (m/s ²)	Gyros (deg/√h)
MEMS	0.002	3
Tactical	0.0006	0.09
Navigation	0.0001	0.0015

The ground truth of the navigation solutions was created from the error-free INS data.

Secondly, the satellite positions for each GNSS system including GPS, GLONASS, GALILEO, COMPASS and QZSS were calculated through Keplerian elements with a 10-degree masking angle. (It should be stated here that such simulated constellations are not related to operational GNSS constellation scenarios). All the GNSS pseudo-ranges were simulated with the standard deviation of one meter.

The examples of simulated GNSS systems were: GPS, GPS/QZSS, BeiDou, Glonass and Galileo. These data sets were first processed individually, and then, in the GNSS/INS intergration scenarios. The Kalman filter (KF) states included three states for each of position, velocity, attitude, gyros, accelerometer plus two states for receiver clock error and drift. The KF states were

updated every second with GNSS pseudo-range measurements.

The analysis of the MDBs for the single fault as well as the correlation analysis for the fault detection statistics in various typical GNSS, and GNSS/INS integration systems are presented below.

4. Numerical Experiments and Analysis

4.1 Single fault scenarios

In order to evaluate the capability of various GNSS systems to detect a faulty pseudo-range, the MDBs defined by Equation (11) were calculated and presented in Figs. (2)-(6).

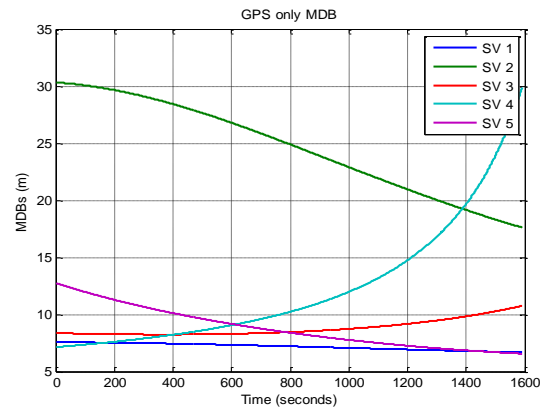


Figure 2: MDBs for GPS Measurements

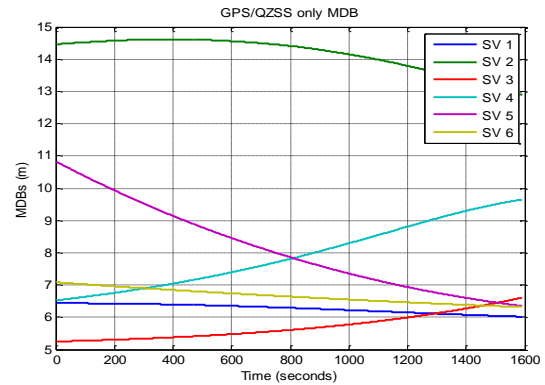


Figure 3: MDBs for GPS/QZSS Measurements

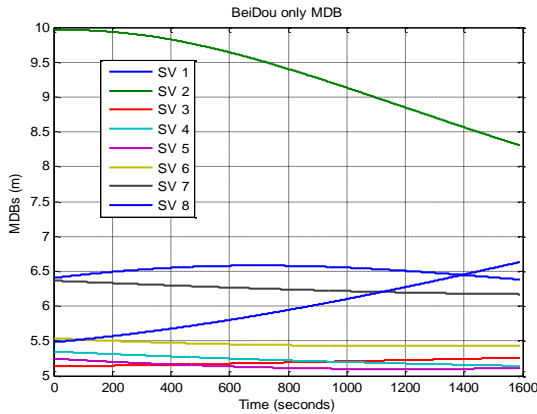


Figure 4: MDBs for BeiDou Measurements

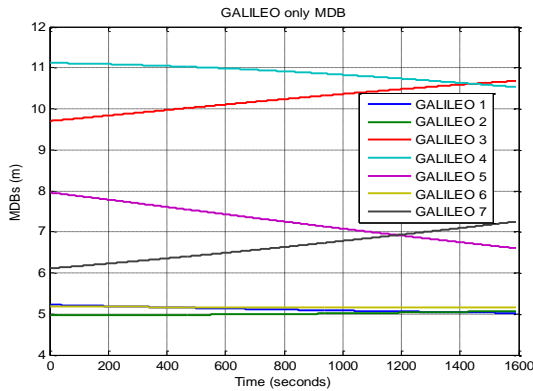


Figure 5: MDBs for Galileo Measurements

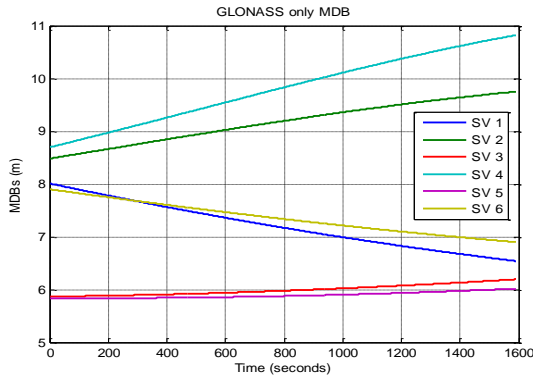


Figure 6: MDBs for Glonass Measurements

From the above figures, it is noted that in the various GNSS constellations simulated here, the MDBs vary from about 5 meters to 30 meters, even with the simulated noise level of 1 meter. These results demonstrated the reality of how difficult it is to detect a fault in the measurements. At the worst situations in the simulated GPS only positioning, a fault could only be detected when its size became large as 30 meters. The MDBs are highly dependent on the number of the satellites tracked and their geometric distributions.

In Figs. (7) to (10), the correlation coefficients between the fault detection statistics for the measurement from SV1 and the rest of the measurements are illustrated for various GNSS positioning scenarios.

In the simulated GPS constellation, there were only 5 SVs. Therefore, there was only one redundant measurement in the positioning solution. As expected, it turned out that all the correlation coefficients between any two fault detection statistics were exactly one! This means that no matter which measurement is the faulty one, all the fault detection statistics will have the same value, which makes the fault identification impossible. Thus, the faults in such a system are inseparable according to both the new separability test (Wang and Knight, 2012) or the multiple hypothesis test (Forstner, 1983; Li, 1986).

The results shown in Fig. 7 demonstrate that, with even one more QZSS satellite combined with GPS, the correlation coefficients can be significantly reduced, but, one of the correlation coefficients was still very close to one over the first 5 minutes.

In the Glonass only positioning scenario, the some correlation coefficients shown in Fig. (10) were very close to one over a long period of time which will result in an extremely weak fault separability.

The correlation coefficients shown in Figs. (8)–(9) also indicate that even with bigger number of SVs tracked, such as 7 SVs for the BeiDou case, and 6 SVs for the Galileo case, the correlation coefficients could reach 0.7–0.8. Such weak geometries for poor fault separability are not rare in satellite navigation. For example, Wang and Knight (2012) demonstrated an even much worse scenario where there were 8 SVs in a positioning solution, but one of the correlation coefficients was as high as 0.9999.

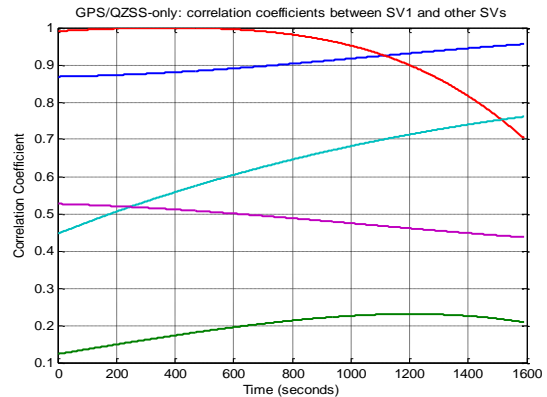


Figure 7: Correlation Coefficients between Fault Detection Statistics in GPS/QZSS Positioning

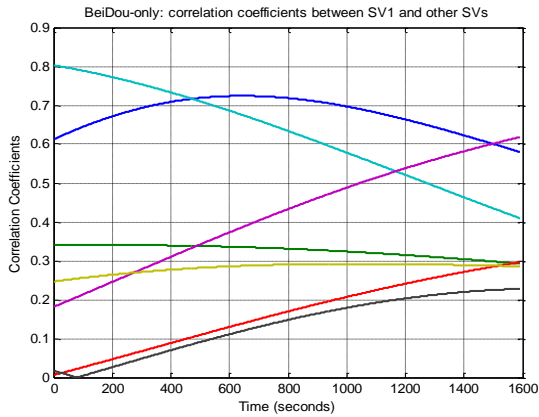


Figure 8: Correlation Coefficients between Fault Detection Statistics in BeiDou Positioning

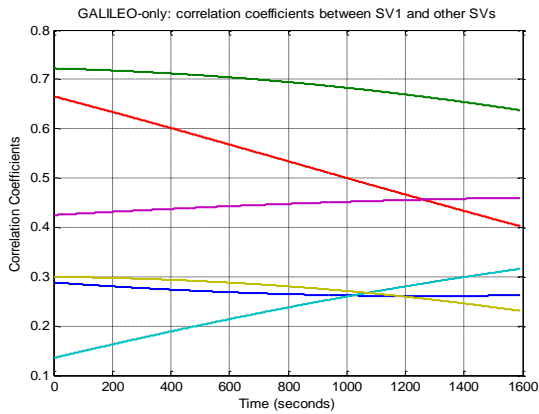


Figure 9: Correlation Coefficients between Fault Detection Statistics in Galileo Positioning

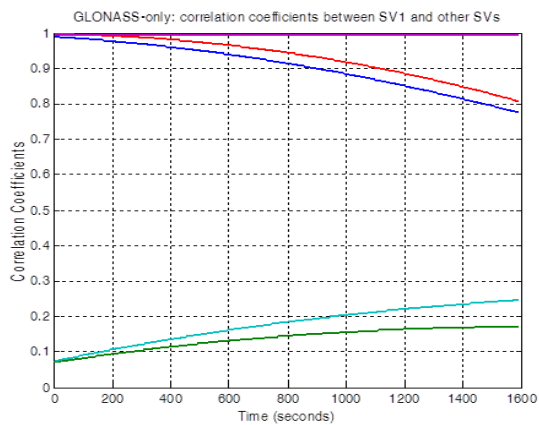


Figure 10: Correlation Coefficients between Fault Detection Statistics in Glonass Positioning

In this research it has been found that with the aiding of INS, through a tight integration of GNSS/INS, both the MDBs for GNSS measurements and the correlation coefficients between faulty measurement detection statistics can be remarkably reduced. The details of these results are illustrated in Figs. (11)-(18).

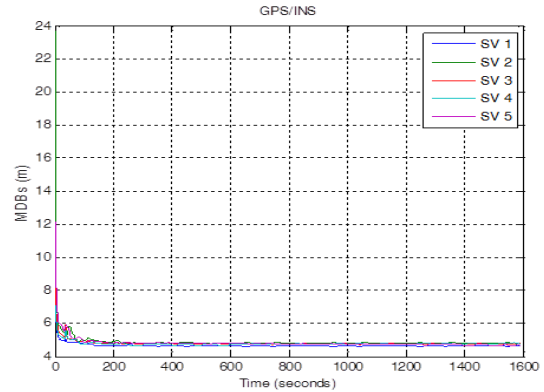


Figure 11: MDBs for GPS Measurements in GPS/INS (Tactical Grade) Integration

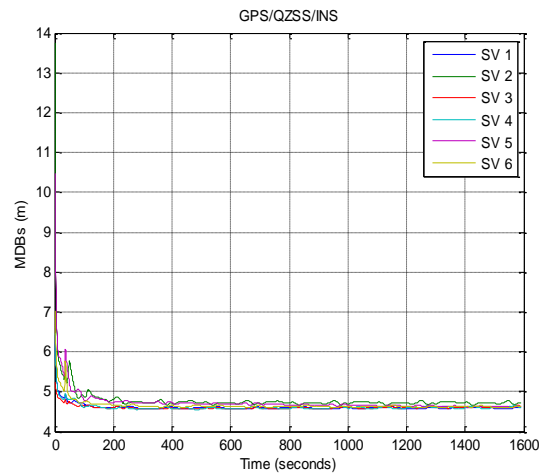


Figure 12: MDBs for GPS/QZSS Measurements in GPS/QZSS/INS (Tactical Grade) Integration

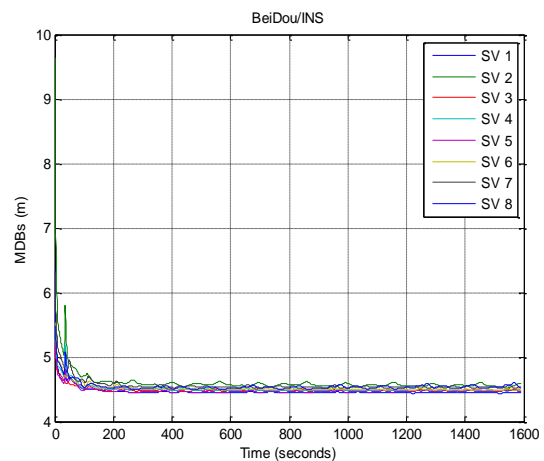


Figure 13: MDBs for BeiDou Measurements in BeiDou/INS (Tactical Grade) Integration

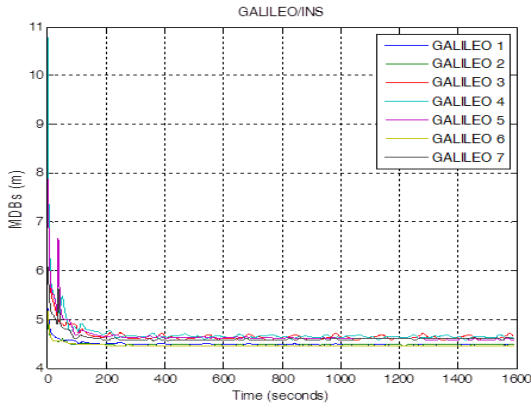


Figure 14: MDBs for Galileo Measurements in Galileo/INS (Tactical Grade) Integration

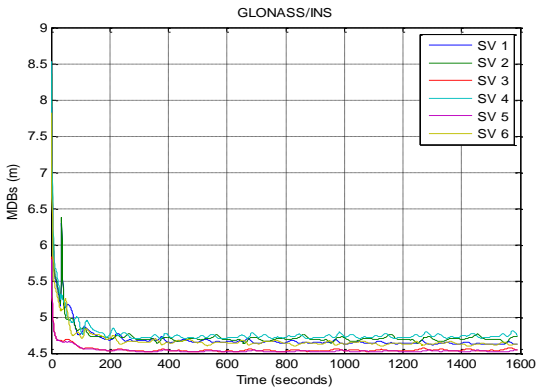


Figure 15: MDBs for Glonass Measurements in Glonass/INS (Tactical Grade) Integration

The MDB results shown in Figs. (11)-(15) have demonstrated the INS sensor can aid GNSS to reduce the MDBs significantly. It is noted that for all the SVs, the MDBs were covered to about 4-5 meters. In Fig.16, similar trends are noted for the maximum correlation coefficients, which were reduced to the range below 0.3.

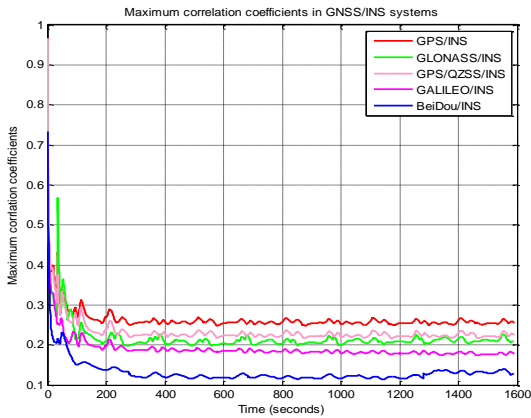


Figure 16: Correlations between Fault Detection Statistics in GNSS/INS (Tactical Grade) Integration

In order to find out the impacts of the IMU sensor noise levels on the MDBs and the correlation coefficients, the GPS/INS integration was carried with simulated MEMS, Tactical and Navigation IMU sensors, respectively. The results illustrated in Figs. (17)-(18) for this simulated trajectory indicate that IMU noise levels do not have a significant impact on the MDBs and correlation coefficients.

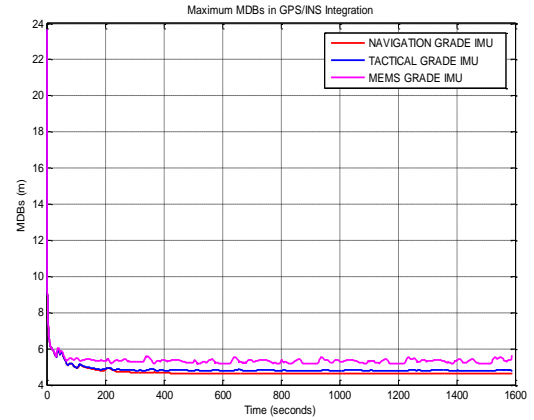


Figure 17: Maximum MDBs in GPS/INS (MEMS, Tactical and Navigation Grades) Integration

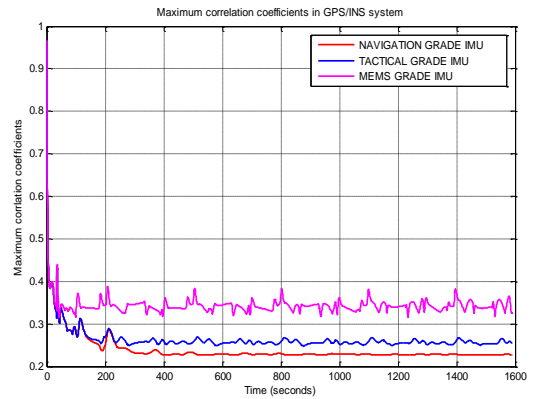


Figure 18: Maximum Correlation between Fault Detection Statistics in GPS/INS (MEMS, Tactical and Navigation Grades) Integration

4.2 Two fault scenarios

Given the PQ_vP matrix and the dimension of faults, which is equal to two in this case, the maximum and global correlation coefficients between the multiple fault detection statistics can be calculated. The numerical results of such correlation coefficients in GPS/INS and GPS/QZSS/INS integration are given below.

A numerical example for equation (18) at epoch 12 in the GPS/INS inetegration is given below:

$$p_{ij} = \begin{bmatrix} 0 & 0 \\ 1 & 0 \\ 0 & 0 \\ 0 & 1 \\ 0 & 0 \end{bmatrix} \begin{bmatrix} 0.081 & -0.018 & 0.010 & 0.008 & -0.018 \\ -0.018 & 0.059 & 0.013 & -0.012 & 0.009 \\ 0.010 & 0.013 & 0.069 & -0.020 & -0.020 \\ 0.008 & -0.012 & -0.020 & 0.053 & 0.010 \\ -0.018 & 0.009 & -0.020 & 0.010 & 0.078 \end{bmatrix} \begin{bmatrix} 1 & 0 \\ 0 & 1 \\ 0 & 0 \\ 0 & 0 \\ 0 & 0 \end{bmatrix} \quad (20)$$

where G_i^θ and G_j^θ correspond to multiple fault test T_i^2 and test T_j^2 for measurement pairs (i) and (j).

One can note that the matrix M for the measurement pair (2, 4) in T_i^2 and (2, 4) in T_j^2 has a diagonal of ones and zeros. In fact, this is true by the definition because it express the correlation coefficients between the measurement pair and itself. Hence the correlation coefficients will inevitably equal to one. The computed correlation coefficients $(Q_{ij})_{Max}$, and $(Q_{ij})_{Global}$, between the multiple fault detection statistics for measurement pair (2, 4) in T_i^2 and all the measurement pairs in T_j^2 are shown in Table 2 below and the similar results are listed in Table 3 for GPS/QZSS/INS integration.

Table 2 Multiple fault detection statistics and correlation coefficients between measurement pair (2, 4) in G_i^θ and all the pairs in G_j^θ in GPS/INS integration

G_j^θ	$(Q_{ij})_{Max}$	$(Q_{ij})_{Global}$	T_k^2
(1,2)	1	0.709	19.80
(1,3)	0.421	0.305	3.29
(1,4)	1	0.726	17.42
(1,5)	0.266	0.245	0.82
(2,3)	1	0.726	25.80
(2,4)	1	1	44.58
(2,5)	1	0.72	20.70
(3,4)	1	0.716	17.82
(3,5)	0.310	0.271	5.08
(4,5)	1	0.717	19.23

It can be clearly seen in Tables 2 and 3 that the correlation coefficients for multiple fault detection cases can be categorized into three groups, i.e., the correlation coefficients between the fault detection statistics for:

- (a) the measurements pairs that share one same measurement, e.g., (2, 4) and each of (1, 2), (1, 4), (2, 3), (2, 5), (3, 4), (4, 5);
- (b) the measurements pairs that do not have any common measurements, e.g., measurement pair (2, 4) and (1, 3), (1, 5) and (3, 5);

(c) the measurement pairs that share the two same measurements, e.g, (2,4) and (2,4).

In the case of the maximum correlation method, one can note that the correlation coefficients between the fault detection statistics for any two measurement pairs in the category (a) are equal to one.

In the case of global correlation approach, however, the correlation coefficients between the fault detection statistics for any two measurement pairs in the category (a) are round 0.7.

In both correlation evaluation methods, the correlation coefficients between the fault detection statistics for those measurements pairs in the category (b) are tiny. In addition, with both approaches the correlation coefficients between the fault detection statistics for the measurement pairs in the category (c) are equal to one because it demonstrates the correlation between the fault detection statistics for the measurement pair and itself. In addition, the maximum correlation coefficients are slightly higher than the associated global correlation coefficients.

In order to show the capability of the system to separate multiple faults in the integrated GNSS/INS systems, two faults of 15m and 13m were added into measurements 2 and 4 respectively, for both GPS/INS, and GPS/QZSS/INS integration. The multiple fault detection statistics as well as the correlation coefficients between measurement pair (2, 4) in G_i^θ and all the pairs in G_j^θ are shown in Tables 2 and 3.

Table 3 Multiple fault detection statistics and correlation coefficients between measurement pair (2, 4) in G_i^θ and all the pairs in G_j^θ in GPS/QZSS/INS integration

G_j^θ	$(Q_{ij})_{Max}$	$(Q_{ij})_{Global}$	T_k^2
(1,2)	1	0.707	18.07
(1,3)	0.373	0.264	0.55
(1,4)	1	0.735	18.87
(1,5)	0.296	0.216	2.56
(1,6)	0.411	0.348	11.65
(2,3)	1	0.707	16.49
(2,4)	1	1	40.50
(2,5)	1	0.710	17.49
(2,6)	1	0.762	25.75
(3,4)	1	0.726	19.63
(3,5)	0.314	0.228	3.81
(3,6)	0.415	0.337	11.36
(4,5)	1	0.714	20.39
(4,6)	1	0.714	22.21
(5,6)	0.434	0.316	14.45

The characteristics of the multiple fault detection statistics in association with the correlation coefficients can be categorized into three groups as follows:

- The first group consists of measurement pair (2, 4) only. Because the faults were injected in those measurement pair, their fault detection statistic value is the highest among other groups.
- The second group are the measurements pairs that include either 2 or 4. Due to the high correlation coefficients between this group and the first group, their fault detection statistic values are quite high.
- The third group are the measurements pairs that include neither 2 nor 4. Their correlation coefficients with the first group is relatively low comparing with the second group, therefore fault detection statistic values are low too.

One can note that the second group is almost fully correlated with the first group especially in the maximum correlation approach case; nonetheless, their fault detection statistic values are not the same as those of the first group. In other words, the rates of change of the fault detection statistic values are not constant. This means that the correlation coefficients between these groups of statistics are not linked with the fault detection statistics proportionally. In the GPS/INS integration (see Table 2), for instance, the correlation coefficients between the measurement pairs (2, 4) and (1, 2) are equal to one. However, the fault detection statistic value of the first pair is 44.58, which is the largest one, while the fault detection statistic for the second pair is only 19.80. Similar situations are noted in Table 3 for the GPS/QZSS/INS integration. But, with a given significance level of 0.1%, and thus, the critical value of the fault test as 13.82, the two simulated fault measurements were detected and identified correctly.

5 Concluding Remarks

Fault detection and identification is an important procedure for use in modern positioning and navigation. The ability of a positioning and navigation system to detect and identify one or multiple faults is highly dependent on the geometric strength of the system.

With the use of the minimal detectable bias (MDB) and the correlation coefficients between the fault detection statistics, the reliability of various GNSS constellations and GNSS/INS integration scenarios have been analysed. Through the simulated data sets, this research has demonstrated some critical reliability issues within a GNSS positioning system with the pseudo-ranges based single point positioning (SPP) mode, particularly at the times when the number of the tracked SVs is low, and the MDBs and correlation coefficients are high. Such critical issues can be well addressed with the use of INS

sensors through the tight integration of GNSS/INS, even with low-cost MEMS sensors.

For multiple fault scenarios, the maximum and global correlation coefficients between the fault detection statistics have been used to analyse the multiple fault separability performances in GPS/INS integration. It has been shown that, for the case of two faults, when the measurement pairs share at least one common measurement, the maximum correlation coefficients between those measurements pairs become one. However, not like the situation of single fault, although the maximum correlation coefficients are exactly one, the successful identification of multiple faults is still possible. This is due to the fact that the rate change of multiple fault detection statistic values is not proportionally related with the maximum or global correlation coefficients. Therefore, such a relationship should be further investigated before the multiple fault separability can be properly related to these correlation coefficients.

References

- Baarda W. (1968) *A testing procedure for sse in geodetic networks*, Netherlands Geodetic Commission, New Series, 2(4).
- Almagbile A. and Wang J. (2011) *Analysis of outlier separability in integrated GPS/INS systems*. IGSS symposium. Sydney Australia 15-17 November.
- Almagbile A., Wang J., Ding W. & Knight N. (2011) *Sensitivity analysis of multiple fault test and reliability measures in integrated GPS/INS systems*. Archives of Photogrammetry, Cartography and Remote Sensing (APCRS), 22, 25-37
- Brenner M. (1995) *Integrated GPS/Inertial Fault Detection Availability*, 9th International Technical Meeting of the Satellite Division of the Institute of Navigation, Kansas City, USA, 1949-1958
- Diesel J. and King J. (1995) *Integration of Navigation Systems for Fault Detection, Exclusion and Integrity Determination – Without WAAS*, ION National Technical Meeting, California, USA, 683-692.
- Förstner W. (1983) *Reliability and discernability of extended Gauss-Markov models*, Deutsche Geodätische Kommission (DGK), Report A, 98, 79-103.
- Hewitson S. and Wang J. (2006) *GNSS Receiver Autonomous Integrity Monitoring (RAIM) performance analysis*, GPS Solutions, 10(3), 155-170.
- Hewitson S. and Wang J. (2007) *GNSS Receiver Autonomous Integrity Monitoring (RAIM) with a*

- dynamic model*, Journal of Navigation, 60(2), 247-263.
- Hewitson S. and Wang J. (2010) *Extended Receiver Autonomous Integrity Monitoring (eRAIM) for GNSS/INS Integration*. Journal of Surveying Engineering, 136(1), 13-22.
- Knight N., Wang, J. and Rizos C. (2010) *Generalized measures of reliability for multiple outliers*, J Geod, 84(4), 625-635.
- Kok J. (1984) *On data snooping and multiple outlier testing*. NOAA Technical Report, NOS NGS.30,USA. Department of Commerce Rockville, Maryland
- Li D. (1986) *Trennbarkeit und Zuverlässigkeit bei zwei verschiedenen Alternativhypothesen im Gauß-Markov-Mödel*. Z.f.Verm,Wesen 111, 114-128
- Nikiforov I. (2002) *Integrity Monitoring for Multi-Sensor Integrated Navigation Systems*, ION GPS 2002, 24-27 September, Portland, OR.
- Ochieng W.Y., Sheridan K.F., Sauer K., Han X., Cross P.A., Lannelongue S., Ammour N. & Petit K. (2002) *An Assessment of the RAIM Performance of a Combined Galileo/GPS Navigation System Using the Marginally Detectable Errors (MDE) Algorithm*, GPS Solutions, 5(3), 42-51.
- O'Keefe K. (2001) *Availability and Reliability Advantages of GPS/Galileo Integration*, ION GPS 2001, Salt Lake City, Utah, September 11-14, 1-10
- Salzmann M. (1993) *Least squares Filtering and Testing for Geodetic Navigation Applications*, Netherlands Geodetic Commission, publications on Geodesy, New Series, Delft, The Netherlands, No. 37, 209 pp.
- Sturza M. A. (1989) *Navigation System Integrity Monitoring Using Redundant Measurements*, Navigation: Journal of the Institute of Navigation, 35(4), 69-87.
- Sorenson H. W. (1970) *Least Squares Estimation: from Gauss to Kalman*, IEEE Spectrum 7, 63-68
- Teunissen P. J. G. (1990) *Quality control in integrated navigation systems*, Proc IEEE PLANS'90, Las Vegas, U.S.A. 158-165
- Wang J. (2002) *Applications of pseudolites in positioning and navigation: Progress and problems*. Journal of Global Positioning Systems, 1(1), 48-56.
- Wang J. and Chen Y. (1999) *Outlier detection and reliability measures for singular adjustment models*. Geomat Res Aust. 71, 57-72
- Wang J., Knight N. and Lu X. (2011) *Impact of the GNSS time offsets on Positioning Reliability*. Journal of Global Positioning Systems, 10(2), 165-172.
- Wang J. and Knight N. (2012) *New Outlier Separability Test and Its Application in GNSS Positioning*. Journal of Global Positioning Systems, 11(1), 46-57.
- Wang J. and Kubo Y. (2010) *GNSS Receiver Autonomous Integrity Monitoring*, In: (Eds. Sugimoto S & R. Shibasaki): GPS Handbook, Asakura, Tokyo, 197-207.
- Wang J., Lee H.K., Hewitson S. and Lee H.-K. (2003) *Influence of Dynamics and Trajectory on Integrated GPS/INS Navigation Performance*. Journal of Global Positioning Systems, 2(2), 109-116.
- Wang J. and Ober P.B. (2009) *On the Availability of Fault Detection and Exclusion in GNSS Receiver Autonomous Integrity Monitoring*. Journal of Navigation, 62(2), 251-261.
- Wang J., Stewart M. and Tsakiri M. (1997) *On quality control in hydrographic GPS surveying*, Third Australian Hydrographic Symposium, 30 November-3December, Fremantle, Western Australia, 1-10.
- Wang J., Xu C. and Wang J.A. (2008) *Applications of robust Kalman filtering schemes in GNSS navigation*. Int. Symp. on GPS/GNSS, Yokohama, Japan, 25-28 November, 308-316.

Biography

Jinling Wang is an Associate Professor in the School of Surveying and Geospatial Engineering, University of New South Wales (UNSW). His major research interests are in the areas of navigation and geospatial mapping with multi-sensors, such as GNSS, INS, cameras. He has published over 200 papers in journals and conference proceedings as well as two commercial software packages (www.gmat.unsw.edu.au/wang). He is a Fellow of the Royal Institute of Navigation (RIN), UK, a Fellow of the International Association of Geodesy (IAG), and is a member of the Editorial Board for the international journal GPS Solutions, Journal of Navigation, International Journal of Navigation and Observations, and President of IAG Sub-Commission 4.2 (2011-2015) on Geodesy in Geospatial Mapping and Engineering. He was elected 2004 President of the International Association of Chinese Professionals in Global Positioning Systems (CPGPS), and the Founding Editor-in-Chief for the Journal of Global Positioning Systems (2002-2007).